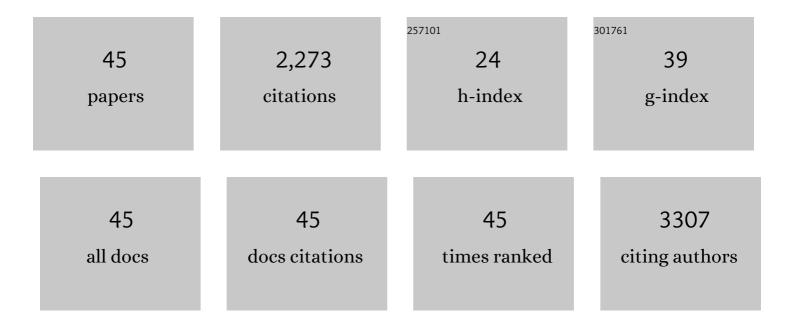
Chae-Ryong Cho

List of Publications by Year in descending order

Source: https://exaly.com/author-pdf/5595135/publications.pdf Version: 2024-02-01



#	Article	IF	CITATIONS
1	Study of diluted magnetic semiconductor: Co-doped ZnO. Applied Physics Letters, 2002, 81, 4020-4022.	1.5	641
2	Room-temperature ferromagnetism in Cr-doped GaN single crystals. Applied Physics Letters, 2002, 80, 4187-4189.	1.5	186
3	Structural reconstruction of hexagonal to cubic ZnO films on Pt/Ti/SiO2/Si substrate by annealing. Applied Physics Letters, 2003, 82, 562-564.	1.5	111
4	Cu Mesh for Flexible Transparent Conductive Electrodes. Scientific Reports, 2015, 5, 10715.	1.6	103
5	Rice-panicle-like γ-Fe2O3@C nanofibers as high-rate anodes for superior lithium-ion batteries. Chemical Engineering Journal, 2019, 356, 60-68.	6.6	98
6	Dielectric and ferroelectric response as a function of annealing temperature and film thickness of sol-gel deposited Pb(Zr0.52Ti0.48)O3 thin film. Journal of Applied Physics, 1999, 86, 2700-2711.	1.1	94
7	Synergistically Enhanced Electrochemical Performance of Hierarchical MoS ₂ /TiNb ₂ O ₇ Hetero-nanostructures as Anode Materials for Li-Ion Batteries. ACS Nano, 2017, 11, 1026-1033.	7.3	89
8	A study of magnetic and optical properties of Cu-doped ZnO. Physica Status Solidi (B): Basic Research, 2004, 241, 1533-1536.	0.7	83
9	Role of reactive gas in atmospheric plasma for cell attachment and proliferation on biocompatible poly É>-caprolactone film. Applied Surface Science, 2008, 254, 5700-5705.	3.1	72
10	Enhanced cycle stability of polypyrrole-derived nitrogen-doped carbon-coated tin oxide hollow nanofibers for lithium battery anodes. Carbon, 2017, 111, 28-37.	5.4	63
11	Flat-surface-assisted and self-regulated oxidation resistance of Cu(111). Nature, 2022, 603, 434-438.	13.7	59
12	Enhanced lithium storage by ZnFe2O4 nanofibers as anode materials for lithium-ion battery. Electrochimica Acta, 2019, 296, 565-574.	2.6	57
13	Dielectric characterization of transparent epitaxial Ga2O3 thin film on n-GaNâ^•Al2O3 prepared by pulsed laser deposition. Applied Physics Letters, 2006, 89, 182906.	1.5	56
14	Effects of Co-doping level on the microstructural and ferromagnetic properties of liquid-delivery metalorganic-chemical-vapor-deposited Ti1â^'xCoxO2 thin films. Applied Physics Letters, 2002, 81, 4209-4211.	1.5	55
15	The structural and optical behaviors of K-doped ZnOâ^•Al2O3(0001) films. Applied Physics Letters, 2004, 85, 419-421.	1.5	52
16	Reversible ferromagnetic spin ordering governed by hydrogen in Co-doped ZnO semiconductor. Applied Physics Letters, 2009, 95, 172514.	1.5	50
17	Electric properties and surface characterization of transparent Al-doped ZnO thin films prepared by pulsed laser deposition. Thin Solid Films, 2008, 516, 5223-5226.	0.8	47
18	Bandgap-designed TiO2/SnO2 hollow hierarchical nanofibers: Synthesis, properties, and their photocatalytic mechanism. Current Applied Physics, 2016, 16, 251-260.	1.1	47

CHAE-RYONG CHO

#	Article	IF	CITATIONS
19	Electrochemical behavior of interconnected Ti 2 Nb 10 O 29 nanoparticles for high-power Li-ion battery anodes. Electrochimica Acta, 2017, 236, 451-459.	2.6	42
20	Copper Better than Silver: Electrical Resistivity of the Grain-Free Single-Crystal Copper Wire. Crystal Growth and Design, 2010, 10, 2780-2784.	1.4	41
21	Solution deposition and heteroepitaxial crystallization of LaNiO3 electrodes for integrated ferroelectric devices. Applied Physics Letters, 1997, 71, 3013-3015.	1.5	40
22	Silicon nanoparticle self-incorporated in hollow nitrogen-doped carbon microspheres for lithium-ion battery anodes. Electrochimica Acta, 2021, 368, 137630.	2.6	30
23	Enhanced cycle stability of iron(II, III) oxide nanoparticles encapsulated with nitrogen-doped carbon and graphene frameworks for lithium battery anodes. Carbon, 2018, 129, 621-630.	5.4	28
24	Electrochemical performance of vertically grown WS2 layers on TiNb2O7 nanostructures for lithium-ion battery anodes. Chemical Engineering Journal, 2020, 382, 122800.	6.6	28
25	Color of Copper/Copper Oxide. Advanced Materials, 2021, 33, e2007345.	11.1	28
26	Surface modification of and selective protein attachment to a flexible microarray pattern using atmospheric plasma with a reactive gas. Acta Biomaterialia, 2010, 6, 519-525.	4.1	14
27	Physicochemical properties and enhanced cellullar responses of biocompatible polymeric scaffolds treated with atmospheric pressure plasma using O2 gas. Materials Science and Engineering C, 2011, 31, 688-696.	3.8	9
28	Lithium Attachment to C60 and Nitrogen- and Boron-Doped C60: A Mechanistic Study. Materials, 2019, 12, 2136.	1.3	9
29	Formation of ferromagnetic Co–H–Co complex and spin-polarized conduction band in Co-doped ZnO. Scientific Reports, 2017, 7, 11101.	1.6	7
30	Abnormally Highâ€Lithium Storage in Pure Crystalline C ₆₀ Nanoparticles. Advanced Materials, 2021, 33, e2104763.	11.1	7
31	Improving the precision of Hall effect measurements using a single-crystal copper probe. Review of Scientific Instruments, 2012, 83, 013901.	0.6	5
32	Wafer-scale high-quality Ag thin film using a ZnO buffer layer for plasmonic applications. Applied Surface Science, 2020, 512, 145705.	3.1	5
33	In Situ Electrochemical Impedance Measurements of α-Fe2O3 Nanofibers: Unravelling the Li-Ion Conduction Mechanism in Li-Ion Batteries. Batteries, 2022, 8, 44.	2.1	5
34	A study of the density of states of ZnCoO:H from resistivity measurements. RSC Advances, 2018, 8, 9895-9900.	1.7	3
35	Growth of AlN Epilayers on Sapphire Substrates by Using the Mixed-Source Hydride Vapor Phase Epitaxy Method. Journal of the Korean Physical Society, 2019, 74, 1160-1165.	0.3	3
36	Inverse Stranski–Krastanov Growth in Single-Crystalline Sputtered Cu Thin Films for Wafer-Scale Device Applications. ACS Applied Nano Materials, 2019, 2, 3300-3306.	2.4	3

CHAE-RYONG CHO

#	Article	IF	CITATIONS
37	Gate voltage-dependent magnetoresistance of Zn _{0.8} Co _{0.2} O:H. RSC Advances, 2016, 6, 97555-97559.	1.7	1
38	Physical properties of as-prepared and post-annealed TiO2 layers by atomic layer deposition and their cell performance. Journal of the Korean Physical Society, 2016, 68, 243-250.	0.3	1
39	Abnormally High‣ithium Storage in Pure Crystalline C ₆₀ Nanoparticles (Adv. Mater.) Tj ETQq1 1 0).784314 r 11.1	gBT /Overlo
40	Effect of reactive gases in an atmospheric-pressure plasma for dye adsorption on ZnO nanorods. Journal of the Korean Physical Society, 2012, 60, 1052-1055.	0.3	0
41	Physical properties of epitaxial Zn1â^'x Cu x O films fabricated by using pulsed laser deposition. Journal of the Korean Physical Society, 2012, 60, 1424-1427.	0.3	0
42	Photonic Crystals: Template-Directed Directionally Solidified 3D Mesostructured AgCl-KCl Eutectic Photonic Crystals (Adv. Mater. 31/2015). Advanced Materials, 2015, 27, 4550-4550.	11.1	0
43	Electrode-Evaporation Method of III-nitride Vertical-type Single Chip LEDs. Journal of the Korean Physical Society, 2018, 73, 1346-1350.	0.3	0
44	Comparison of AIN Nanowire-Like Structures Grown by using Mixed-Source Hydride Vapor Phase Epitaxy Method. Journal of the Korean Physical Society, 2019, 75, 242-247.	0.3	0
45	Growth of a Thick AlN Epilayer by Using the Mixed-Source Hydride Vapor Phase Epitaxy Method. Journal of the Korean Physical Society, 2020, 77, 282-287.	0.3	0